

ORIGINAL PAPER

EPITHELIAL MESENCHYMAL TRANSITION AND CANCER STEM CELL MARKERS IN ORAL EPITHELIAL DYSPLASIA AND ORAL SQUAMOUS CELL CARCINOMA

BURCU TOKOZLU^{1#}, ÖZLEM ÖZER YÜCEL^{1#}, SIBEL E. GÜLTEKİN¹, LEYLA ARSLAN BOZDAĞ²

¹Department of Oral Pathology, Faculty of Dentistry, Gazi University, Ankara, Turkey

²Department of Biology, Faculty of Dentistry, Gazi University, Ankara, Turkey

[#]These authors contributed equally to this work.

The role of cancer stem cells (CSC) in oral cancer is widely accepted. Yet, the existence of CSC in dysplastic tissue and the molecular pathways of progression from dysplasia to malignancy remain to be explored.

Our retrospective study aimed to analyze the presence of CSC in oral epithelial dysplasia and oral squamous cell carcinoma (OSCC) concerning two epithelial-mesenchymal transition markers: Snail and E-cadherin. Formalin-fixed, paraffin-embedded tissue samples of oral epithelial dysplasia (OED), OSCC, and oral epithelial hyperplasia (OEH) were used. Immunohistochemistry and quantitative RT-qPCR detected the expression of Snail and CD133, whereas CD44 and E-cadherin were evaluated solely immunohistochemically.

OSCC cases showed significantly higher CD133 immunoreactivity and inflammation scores and significantly decreased E-cadherin expression compared to OED and OEH groups. Snail mRNA up-regulation was seen in 100% of the OSCC cases followed by 85% for OED cases and 82.5% OEH cases among those that displayed positive mRNA expression by RT-qPCR.

The Snail upregulation in all OSCC cases proves that Snail plays a significant role in oral cancer. Our results also suggest that CD133 and E-cadherin may be potential diagnostic markers in oral cancer progression.

Key words: cancer stem cells, epithelial mesenchymal transition, oral squamous cell carcinoma, Snail, oral epithelial dysplasia.

Introduction

Head and neck squamous cell carcinoma, which includes malignancies originating from the oral cavity, pharynx and larynx, are a heterogeneous group of tumors with variable presentation. Over 90% of oral cancers originate from the squamous epithelium lining the oral cavity. The data of GLOBOCAN 2020 indicate 377,713 new oral cancer cases worldwide [1].

The majority of patients present at diagnosis with loco-regionally advanced disease (stage III–IV), which results in poor prognosis [2, 3]. Oral squamous cell carcinoma (OSCC) still remains a cancer associated with a high mortality rate, despite the new molecular advances in the field.

Oral cancer can arise *de novo*, or following a pre-malignant phase clinically and microscopically [4]. Identification and treatment of precursor lesions with

high risk of malignant transformation are important in order to prevent development of OSCC. Although the concept of stepwise transition from oral premalignant lesions to OSCC has been well established [5], it is difficult to predict both the probability and the duration of the malignant transformation [6]. Therefore, numerous studies have aimed to define new and more reliable molecular diagnostic/prognostic markers and validate novel therapeutic targets [7].

There is emerging evidence that cancer stem cells (CSCs) drive and maintain tumor growth. The CSC hypothesis posits that only a sub-population of cancer cells has the capacity to proliferate indefinitely and drive tumorigenesis [8–10]. CSCs have been identified in leukemia [11], and more recently in many solid tumors including those of the breast, brain, and head and neck [12]. Ishizawa *et al.* [13] suggested that fewer than 1/2500 CSCs were present in head and neck tumors. Among a number of markers, CD133, CD44, beta-1 integrin, CD71, E-cadherin, and beta-catenin are the most common CSC markers that have been studied in OSCC [12]. However, reliable molecular markers defining CSCs in oral epithelial dysplasia and OSCCs still remain to be explored.

The overall aim of our study is to determine epithelial-mesenchymal transition (EMT) and CSC associated mRNA expression levels during the process of transition from “oral epithelial dysplasia” (OED) to OSCC in order to establish a potential diagnostic marker. For this purpose, we analyzed EMT-CSC interaction by evaluating:

- Snail, E-cadherin, CD133 and CD44 levels immunohistochemically in paraffin-embedded archival tissue specimens diagnosed as OED, OSCC and “oral epithelial hyperplasia” (OEH);
- Snail and CD133 mRNA expression by quantitative RT-PCR in paraffin-embedded archival tissue specimens mentioned above;
- correlations between Snail, E-cadherin, CD133 and CD44 levels and histopathological parameters.

Material and methods

Tissue specimen histological and clinical data

This study included a total of 58 formalin-fixed, paraffin-embedded (FFPE) tissue samples of OED ($n = 23$), OSCC ($n = 16$) and OEH ($n = 19$) between the years of 2010 to 2015, used from the archive of the Department of Oral Pathology Faculty of Dentistry, Gazi University, Ankara, Turkey. The experimental protocol was reviewed and approved by the Ethics Committee of Gazi University (142/07102013).

Microscopically, all tissue sections were re-reviewed and graded by three oral pathologists (S.E.G.,

O.O.Y and B.T.) using hematoxylin and eosin (H&E) stained sections.

OSCC cases were graded as “poor”, “moderate” or “well” differentiated according to the WHO criteria [14]. OED cases were classified as “low” or “high” grade using a binary grading system [15]. OEH cases served as controls. Inflammation in all cases was graded as low, moderate and high with scores of 1, 2 and 3 respectively [16–18].

Immunohistochemical analysis

FFPE tissues were cut in 4- μ m sections and immunostained by the standard avidin-biotin-peroxidase complex method. After deparaffinization, antigen retrieval was performed using EDTA for 30 min for CD133 and Snail; and 60 min for CD44 and E-cadherin antibodies. For detection of specific immunoreactivity, the specimens were incubated with monoclonal antibodies against CD133 (rabbit polyclonal, Proteintech Europe), CD44 (Leica, NCL-CD44 mouse monoclonal, df1485, Newcastle, United Kingdom), Snail (rabbit polyclonal, Thermo Scientific) and E-cadherin (Leica, mouse monoclonal, 36b5, Newcastle, United Kingdom). Immunohistochemical staining was performed using VENTANA BENCHMARK X (Ventana Medical Systems, Inc. 1910 E. Innovation Park Drive, Tucson, Arizona, USA). Optimal dilutions were 1/100 for CD133, CD44, and E-cadherin, whereas Snail was diluted to 1/50. Gill’s hematoxylin was used for counterstaining. Bluing Reagent (VENTANA) was applied for post-counterstaining. The positive control for Snail was breast invasive ductal carcinoma tissue. Colon mucosa served as a positive control for both CD44 and CD133. The positive control for E-cadherin was gingival epithelium. All controls gave satisfactory results.

The evaluation of immunoreactivity was performed by two pathologists (SEG, O.O.Y, and BT) under $\times 200$ magnification on a Leica QWin Plus v3.3.1 (Leica Microsystems GmbH, Wetzlar, Germany), including all the tumor tissue for SCC cases, and all the epithelial area for dysplasia and hyperplasia cases. Nuclear staining was accepted as positive for Snail immunoreactivity. The H score was used for evaluation when the immunoreactivity of the cells was assessed for both the staining intensity and the percentage of tumor or normal cells stained (Table I) [19].

Membranous staining was accepted as positive for CD44 and E-cadherin. The percentage of immunostained cells for E-cadherin was scored as 0 = no stained cells, 1 (less than 10%), 2 (10–75%), or 3 (more than 75%) [3].

The percentage of immunostained cells for CD44 was scored as 0 = no stained cells, 1 (less than 10%), 2 (10–50%), or 3 (more than 50%). Both membranous and cytoplasmic staining were accepted as positive for CD133. The percentage of immunostained

Table I. Evaluation of Snail immunoreactivity by H score

STAINING INTENSITY	PERCENTAGE OF STAINING CELLS	H SCORE (INTENSITY × PERCENTAGE)	SCORE
0	Less than 1% (0)	0	0
1	1–40% (1)	1–2	1 (low)
2	40–80% (2)	3–4	2 (moderate)
3	More than 80% (3)	6–9	3 (heavy)

cells for CD133 was scored as 0 (less than 5%), 1 (5–50%), or 2 (more than 50%) [3, 20].

RT-qPCR analysis

Deparaffinization of FFPE tissue and total RNA isolation:

Depending on the size of the tissue sample, one or two paraffin sections (10 μ m thick) were used for the isolation of RNA. The sections were cut and immediately placed in a 1.5 ml tube, in duplicates for each sample. The FFPE tissue samples were deparaffinized with xylene (800 μ l) at 37°C for 2 hours. Then tubes were centrifuged twice at 7000 rpm for 2 minutes at room temperature. These steps were followed by the removal of the supernatant and supplementation of 100% EtOH (400 μ l) to the precipitated tissue. Tubes were centrifuged at 7000 rpm for 2 minutes at room temperature. Subsequently, EtOH was carefully discarded without disturbing the pellet and EtOH washing was repeated twice. Finally, residual EtOH was entirely removed and the pellet was left to dry for 25 minutes at room temperature.

Total RNA was extracted using the High pure FFPET RNA Isolation Kit (Roche Diagnostics, Mannheim and Penzberg, Germany) according to the manufacturer's protocol. In brief, 100 μ l of RNA tissue lysis buffer (Roche Diagnostics) and 16 μ l of 10% SDS solution were added to the deparaffinized tissue, sequentially. Samples were incubated with Proteinase K (40 μ l) for 30 min at 85°C, then cooled down to 50°C, followed by additional treatment with 80 μ l of Proteinase K. After several washing steps, nucleic acids were eluted in the elution buffer. This was followed by DNase I treatment and the final washing steps. The final isolate was obtained after the addition of RNA elution buffer. The purity and concentration of total RNA were determined by measuring the absorbance at 260 nm and 280 nm using the PROMEGA Quantus Fluorometer. All steps in the preparation and handling of total RNA were conducted in a laminar flow hood under RNase free conditions. The isolated total RNA was stored at –80°C until used for cDNA synthesis.

cDNA synthesis

Complementary DNA (cDNA) was synthesized using a Transcriptor High Fidelity cDNA Synthesis Kit (Roche Diagnostics, Mannheim and Penzberg,

Germany). Before the reverse transcription process, 1 μ l of random primer, 1 μ l of oligoprimers, and 9.4 μ l of RNA were mixed together. The reaction mixture was incubated at 65°C for 5 min, and then quickly chilled on ice. Subsequently, an additional mixture of 4 μ l of reverse transcriptase buffer, 0.5 μ l of RNase inhibitor, 2 μ l of DNTP solution, 1 μ l of DTT and 1 μ l of reverse transcriptase solution was prepared and added to the reaction mixture in PCR tubes. The cDNA synthesis reaction was performed at 55°C for 30 min, 85°C for 5 min in order to obtain a 20 μ l volume of cDNA.

RT-qPCR

The mRNA expression levels of Snail and CD 133 genes were measured by RT-qPCR. The Snail gene (LOT 90017736, Roche Diagnostics, Mannheim, Germany) primer sequences are as follows: 5'-TGCA-GGACTCTAATCCAAGTTTACC-3' (forward) and 5'-GTGGGATGGCTGCCAGC-3' (reverse). CD133 (LOT 90017737, Roche Diagnostics, Mannheim, Germany) primer sequences are as follows: 5'-TTTC-AAGGACTTGCGAACTCTCTT-3' (forward) and 5'-GAACAGGGATGATGTTGGGTCTC-3' (reverse). The beta-actin gene was used as a housekeeping gene (ACTB, LOT 0000001025 Roche Diagnostics, Mannheim, Germany).

The mRNA expression levels were detected by employing TaqMan probes using the real-time RT-qPCR LightCycler-16258 PCR system (Roche Diagnostics, Mannheim and Penzberg, German). The RT-qPCR Taq Man assay was carried out with the LightCycler 480 Probe Master according to the manufacturer's recommendations. Real-time PCR amplification for each gene mRNA was performed using a total volume of 20 μ l that contained 10 μ l of 2 × PCR probes master, 4 μ l of H₂O, 5 μ l cDNA, 1 μ M for each primer TaqMan probe mixture. Positive and negative controls were included throughout the procedure. Cycle conditions of the relative qRT-PCR were preincubated at 95°C for 10 min, followed by 50 amplification cycles of 60°C for 30 s, 72°C for 1 s and cooling at 40°C for 30 s. The mRNA expression level was quantified by determining the cycle threshold (CT), which is the number of PCR cycles required for the fluorescence to exceed a value significantly higher than the background fluorescence.

Statistical analysis

The data were transferred to the IBM SPSS Statistics 23 program and analyses were completed. Frequency analysis (n , %) was used for categorical variables and descriptive statistics were used for continuous variables.

In our study, nonparametric statistical methods were used because $n < 30$. The Mann-Whitney U test was used to analyze the difference between two independent groups and the Kruskal-Wallis test was used to analyze the difference between more than two independent groups. Spearman's rho correlation coefficient was used to analyze the relationship between continuous variables. The relationship between two categorical variables was determined by the χ^2 test.

Results

Patient demographics and histological grading

Patient demographics and clinical data are summarized in Tables II and III.

No statistically significant differences were found for the distribution of age and gender among the groups. Buccal mucosa was the common anatomic site for both the OED and OSCC cases, whereas most of the OEH cases were located on the floor of the mouth. Out of 23 OED cases, 9 were diagnosed as low grade (LG), and 14 were diagnosed as high grade (HG). Most of the OSCC cases were graded as well-differentiated.

Table II. Distribution of demographic and clinical data among the groups

	OEH, $N = 19$		OED, $N = 23$		OSCC, $N = 16$	
	N	%	N	%	N	%
Gender						
Male	8	42.1	11	47.8	6	37.5
Female	11	57.9	12	52.2	10	62.5
Localization						
Floor of mouth	0	0.0	2	8.7	2	12.5
Buccal mucosa	4	21.1	5	21.7	4	25.0
Tongue	1	5.3	4	17.4	3	18.8
Maxilla	5	26.3	7	30.4	3	18.8
Mandibula	9	47.4	5	21.7	4	25.0
	MEAN \pm SD	MIN.-MAX.	MEAN \pm SD	MIN.-MAX.	MEAN \pm SD	MIN.-MAX.
Age (years)	48.27 \pm 14.28	20–75	55.22 \pm 15.42	26–80	59.46	37.90 \pm 15.07

OED – oral epithelial dysplasia, OEH – oral epithelial hyperplasia, OSCC – oral squamous cell carcinoma

Table III. Snail, E-cadherin, CD44 and CD133 immunoreactivity

AB	OEH		OED		OSCC		P
	N	%	N	%	N	%	
Snail							
Low expression	14	73.7	22	95.7	11	78.6	0.095
High expression	5	26.3	1	4.3	3	21.4	
E-cad							
E-cadherin loss	8	44.4	17	73.9	15	93.8	0.006*
Normal	10	55.6	6	26.1	1	6.3	
CD44							
Negative	3	15.8	4	17.4	1	6.3	0.541
Positive	16	84.2	19	82.6	15	93.8	
CD133							
Negative	15	83.3	17	73.9	7	46.7	0.063
Positive	3	16.7	6	26.1	8	53.3	

* $p < 0.05$

OED – oral epithelial dysplasia, OEH – oral epithelial hyperplasia, OSCC – oral squamous cell carcinoma

Regarding all the groups, most of the samples included varying degrees of mononuclear inflammatory cell infiltration in the lamina propria. Mean inflammation scores were detected as 1.3, 1.9 and 2.1 in OEH, OED and OSCC cases, respectively, and the score was significantly higher in the OSCC cases ($p = 0.022$).

Immunohistochemistry

Snail

Positive immunoreactivity was evidenced in all groups with different percentage values. The immunoreactivity pattern displayed positive nuclear staining in both epithelial cells and connective tissue cells in the lamina propria in OEH and OED cases with prominence in basal keratinocytes, inflammatory cells, and fibroblasts in the lamina propria. 26.1% of OED cases had a score of 0, 69.6% had a score of 2, whereas 4.3% showed positive immunostaining with a score of 3. OSCC cases showed positive immunoreactivity predominantly at the periphery of tumor islands, and infiltrating tumor cords and strands. Especially poorly differentiated tumor parenchyma was observed to exhibit intense nuclear immunostaining. 14.3% of OSCC were evaluated with a score of 1, 14.3% with a score of 2, and 7.1% with a score of 3 (Fig. 1).

E-cadherin

E-cadherin loss was evident in 44.4% of OEH cases, 73.9% of OED cases and 93.8% of OSCC cases. The mean immunoreactivity score values for E-cadherin were found to be significantly lower in OSCC cases (1.3), decreasing gradually compared to OED (2.5) and OEH (2.0) cases ($p = 0.006$) (Fig. 1).

CD44

The membranous immunoreactivity pattern for CD44 was observed in OEH cases principally in basal and suprabasal layers extending until two-thirds of the epithelium. In contrast, dysplastic epithelium displayed weak CD44 staining in basal and parabasal layers; moreover, budding rete-pegs also showed weak immunoreactivity for CD44 (Fig. 1A,B). 17.4% of OED cases scored 0, 39.1% scored 1, 34.8% scored 2, whereas 8.7% showed positive immunostaining with a score of 3. 6.3% of OSCC were evaluated with a score of 0, 25% with a score of 1, 50% with a score of 2, and 7.1% with a score of 3. Mean levels were detected as 1.5, 1.3 and 1.8 for OEH, OED and OSCC cases, respectively. No statistically significant differences were found among the groups (Fig. 1).

CD133

CD133 immunoreactivity was positive in 16.7% of OEH cases. The expression pattern was membra-

nous and cytoplasmic, predominantly in basal and suprabasal keratinocytes (Fig. 2A,B). Dysplastic epithelium OED cases showed positive immunostaining in rete-pegs in the basal layer. A few cases showed positive stained cells extending to the spinous and granular layers (Fig. 2C). 26.1% of OED and 57% of OSCC cases were immunolabeled as positive. The mean percentage of immune positive cells varied from 6.7 to 46.7% in OSCC cases. Membranous staining was observed as positive at the periphery of tumor islands, and inflammatory cells in tumor stroma. Mean values for CD133 scores for OEH, OED, and OSCC groups were found to be 0.2, 0.3, and 0.6, respectively. The OSCC group was found to have significantly higher CD133 immunoreactivity levels ($p < 0.05$) (Fig. 1).

Histopathologic correlation

Snail and CD133 immunoreactivity were positively correlated in OEH cases ($p < 0.05$, $r = 0.469$). A strong positive correlation was detected between CD133 immunoreactivity and inflammation score in OSCC cases ($p < 0.05$, $r = 0.661$).

No statistically significant correlations were found between immunoreactivity levels and histopathological parameters such as tumor differentiation or histological grading regarding OSCC and OED cases in any marker.

RT-PCR

Snail

Relative Snail mRNA expression was detected in 50% of OSCC cases, 60.9% of OED cases and 89% of OEH cases, where the difference between OEH and OSCC groups was statistically significant ($p = 0.033$).

Regarding the fold change in Snail mRNA levels, all positive OSCC cases ($n = 8$) showed increased mRNA expression (Fig. 2). In the OED group, out of 23 cases 14 were detected to have positive mRNA expression where 12 cases showed increased expression and 2 cases displayed decreased expression. The mean percentage of cases with increased mRNA expression was found to be 85% (Fig. 3). Similarly, the mean percentage with increased mRNA expression in OEH cases was 82.5% (Fig. 4). Out of 15 OEH cases, 12 showed increased mRNA expression, 2 showed decreased expression and 2 displayed no expression. Snail mRNA expression levels did not differ significantly among the groups ($p > 0.05$).

CD133: Regarding all the groups, CD133 mRNA expression was detected in one case out of 16 OSCC cases, and two cases out of 23 OED cases. The data for CD133 mRNA levels were insufficient to perform statistical analysis.

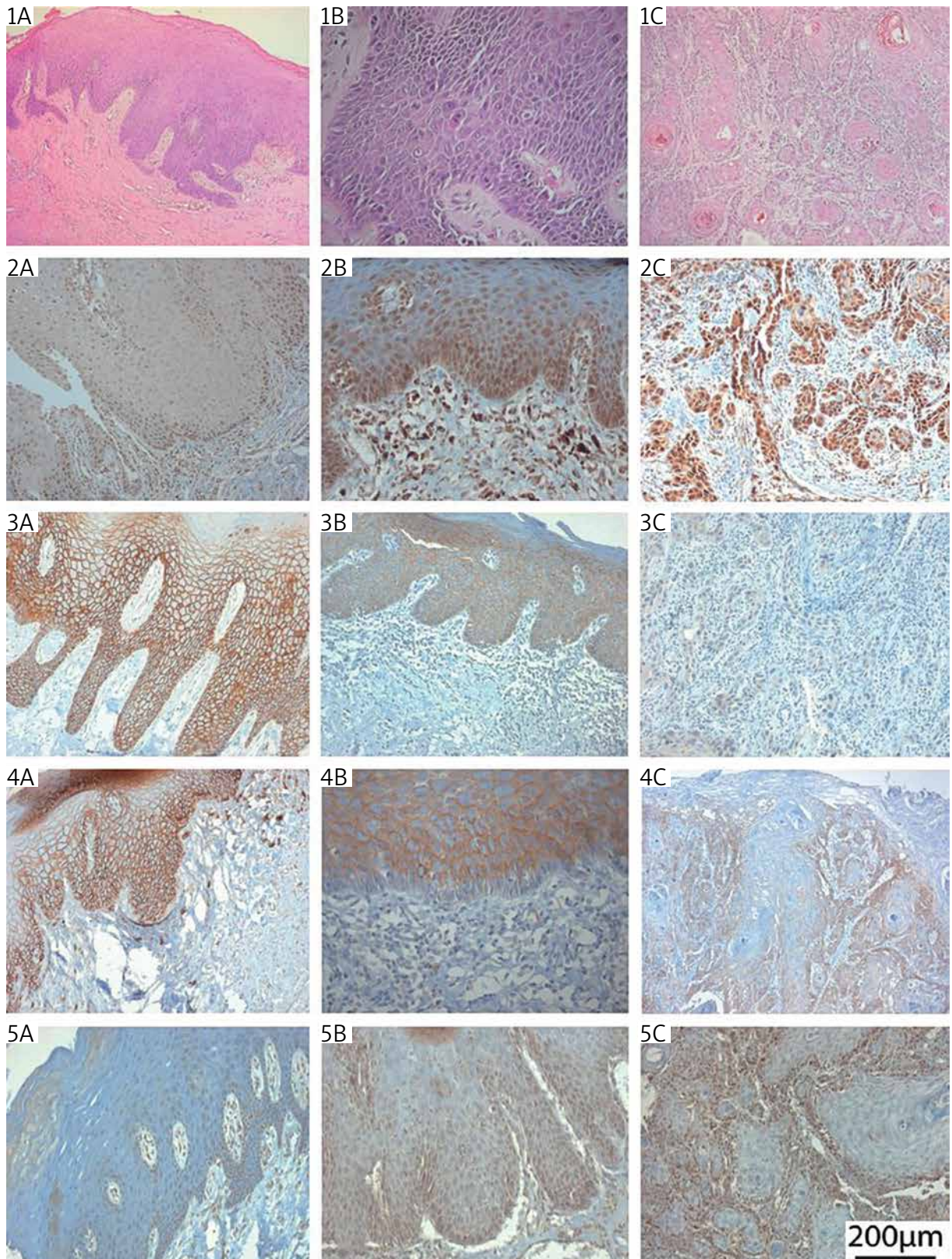


Fig. 1. Representative images showing histological characteristics of oral epithelial hyperplasia (OEH) (A), oral epithelial dysplasia (OED) (B), and oral squamous cell carcinoma (OSCC) (C) on H&E (1) staining and the immunohistochemical expression of Snail (2), E-cadherin (3), CD44 (4), and CD133 (5). Images were exported from Leica QWin Plus v3.3.1 (Leica Microsystems GmbH, Wetzlar, Germany) image analyze program, scale bar = 200 μ m. Quantification of immunostaining showed significant e-cadherin decreasing in OSCC cases gradually compared to OED and OEH cases (3A-C). The OSCC group was found to have significantly higher CD133 immunoreactivity levels

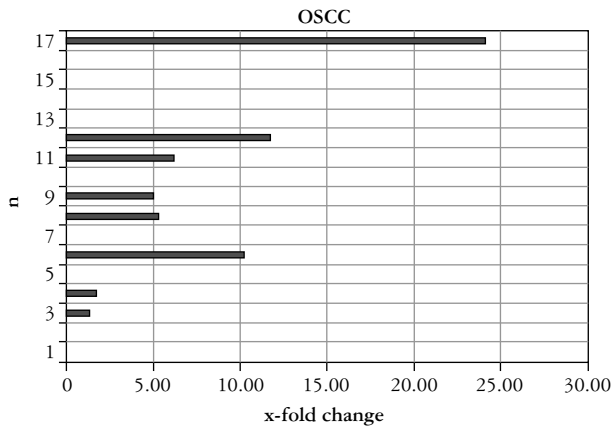


Fig. 2. Relative Snail mRNA expression in oral squamous cell carcinoma cases

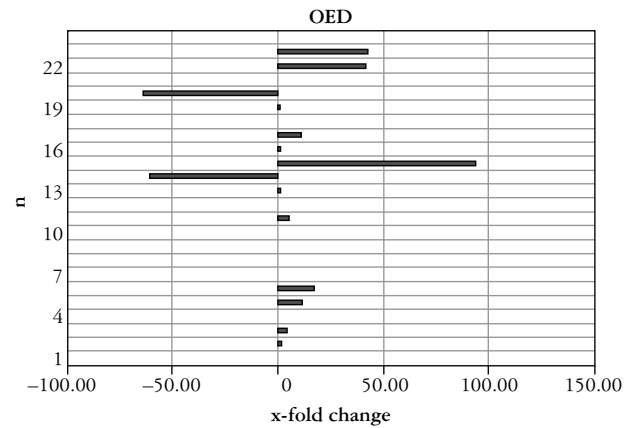


Fig. 3. Relative Snail mRNA expression in oral epithelial dysplasia cases

Discussion

Oral cancer is one of the most common cancers with high mortality and morbidity rates, and more than 50% of patients are diagnosed in advanced stages. A number of OSCC cases arise de novo, whilst others may develop from the preexisting dysplasia of the oral mucosa [21]. Therefore, it is of great importance to determine the factors that influence the cancer invasion process, especially in lesions at the “precancerous” stage. In recent years, the role of EMT constituents through the sequence of oral dysplasia to OSCC has been investigated, demonstrating it to be an important process in carcinogenesis that is directly associated with the aggressiveness of OSCC. Elucidation of the molecular mechanisms in this process may contribute to the introduction of these potential markers into routine laboratory diagnostics. The identification of markers associated with the progression of oral epithelial dysplasia is of paramount importance for establishing a possible relationship with the prognosis of these lesions [22]. From this point of view, we designed our study based on materials consisting of tissues diagnosed as “hyperplasia”, “dysplasia” and “squamous cell carcinoma” in order to evaluate the effect of Snail expression on E-cadherin, CD133, and CD44 immunoreactivity.

The results of our study showed that the mean inflammation score, which is among the histopathological parameters, was significantly higher in the SHC group compared to the other groups. Recent scientific studies have revealed the relationship between chronic inflammation and carcinogenesis [23]. DNA and tissue damage caused by chronic inflammation and genetic and epigenetic changes that occur in this process trigger carcinogenesis [24]. It has been shown that pro-inflammatory cytokines such as IL-1, IL-8 and growth factors such as TGF- β , which have been shown to be expressed by keratinocytes as well as inflammatory cells in tissues during chronic inflamma-

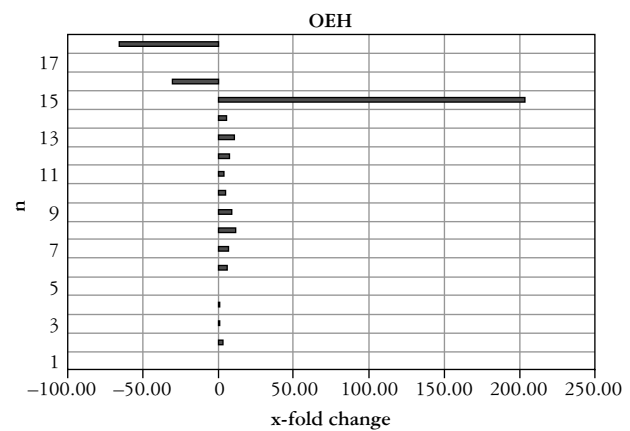


Fig. 4. Relative Snail mRNA expression in oral epithelial hyperplasia cases

tion, may be effective in carcinogenesis [25, 26]. One of the main factors involved in tumor progression is the pro-inflammatory cytokine TNF α , produced by macrophages. TNF α also has a crucial role in EMT as it induces overexpression of the transcription factor Snail, leading to downregulation of E-cadherin and upregulation of N-cadherin, which are among the key molecules involved in EMT [27].

In our study we evaluated the expression of Snail using both immunohistochemical and PCR techniques. We detected Snail immunoreactivity generally as more intense in the periphery of tumor islands and in poorly differentiated areas. It has been reported that this expression pattern in SHC cases may have prognostic value for invasion and metastasis. Tumor budding refers to the grouping of single or up to five cells in the invasive area of the tumor, and it is suggested that these areas are a strong marker for lymph node metastasis [28, 29]. In dysplasia cases, positivity was observed mostly in areas showing budding and polarization loss. Studies have shown that the loss of epithelial polarity in the EMT process affects the functions of polarity complexes and subsequently cell-cell integrity. In particular, Snail and ZEB1 have been

shown to play an important role in this process [30]. This information explains the morphological localization of Snail expression pattern in dysplasia and SHC cases. When relative Snail mRNA expression was evaluated in our study, increased expression levels were observed in some cases and decreased in others in the dysplasia and EH groups, while increased expression levels were found in all SHC cases with positive Snail mRNA. However, no statistically significant difference was found between the groups.

Immunohistochemical studies have reported that E-cadherin immunoreactivity is reduced in many cancers, including head and neck cancers and oral cancer [31, 32]. It is known that loss of E-cadherin expression on the invasive surface of the tumor in oral cancer is important in tumor progression and tumors with E-cadherin loss have a poor prognosis [33]. In our study, a significant decrease in E-cadherin immunoreactivity was observed especially in areas where the tumor infiltrated as smaller cell groups and around sub-mucosa and muscle invasion. Our findings, in parallel with the literature, support the view that loss of E-cadherin is a marker of malignancy. E-cadherin inactivation in cancers may lead to invasive growth by causing marked phenotypic changes in cell-cell contacts [34]. In our study, when all groups were evaluated together, E-cadherin loss was observed in 75% of the cases with increased Snail mRNA. However, in parallel with the findings of Rosivatz *et al.* [35], no correlation was found between Snail expression and E-cadherin loss.

Takunen *et al.* [30] reported that Snail as well as EMT factors such as ZEB1 and ZEB2 suppressed E-cadherin expression in cells isolated from primary oral squamous cell carcinoma; they suggested that EMT may be triggered independently of Snail in oral cancer. In addition, podoplanin-mediated actin remodeling has been reported to be effective in the invasion process in SCLCs together with EMT [36].

Many CSC markers have been identified in oral SCLCs to date. Some of these are cell surface molecules and some are transcription factors [12]. Among the cell surface molecules are CD133, CD44, and CD90, CD24. Many researchers argue that these surface molecules may be useful in identifying cancer-initiating cells [37, 38]. One of the prominent findings of our study was that CD133 immunoreactivity was significantly higher in OSCC cases compared to the EH group ($p = 0.05$). Positive CD133 immunoreactivity was observed in 16% of the cases in the EH group, 27% in the dysplasia group and 53% of the OSCC cases. In parallel with our findings, Ravindran *et al.* [39] reported that CD133 immunoreactivity increased relatively in the sequence from oral epithelial dysplasia to oral cancer and showed co-expression with Musahi-1. In another immunohistochemical study, it was reported that CD133 im-

munoreactivity increased up to 60% in tumor cells in oral cancer [40].

When CD133 mRNA expression levels were evaluated, an increase was observed in one case in the OSCC group and in two cases in the dysplasia group. CD133 mRNA expression could not be determined in other cases in all groups. These data do not indicate the absence of CD133 protein expression changes in dysplasia and cancer. The reliability of mRNA levels as indicators is proportional to their matching at the protein level [41]. In our study, this mapping was performed by immunohistochemistry and positive expression was detected in 29% of the cases (3 in the EH group, 6 in the dysplasia group, and 8 in the OSCC group). *In vitro* studies have shown that 1–3% of tumor cells express CD133 in oral cancer [10]. The fact that it is expressed less than other cell surface markers, case selection and methodological differences may be the reasons that CD133 expression could not be demonstrated *in vivo*.

Another significant finding of our data was the strong positive correlation between CD133 immunoreactivity and inflammation score in OSCC cases ($p < 0.05$, $r = 0.661$). The relationship between the inflammation and the CSCs was clearly shown in the development and progression of the cancer. In a recent study, Awasthi *et al.* [42] reported a direct correlation of IL-1 β levels with immunohistochemistry scoring in OSCC cases, demonstrating a significant role for CD44 and CD133 positivity in the increase of IL-1 β levels. Taking all the evidence together, we may speculate that CD133 may play an important role in tumor development in the context of the inflammation – dysplasia – carcinoma sequence.

Positive CD44 immunoreactivity was observed in 84% of the cases in the EH group, 83% in the dysplasia group and 94% of the SHC cases. Although the mean values of CD44 immunoreactivity increased gradually from hyperplasia and dysplasia cases to SHC, no statistically significant difference was found. In parallel with our findings, Margaritescu *et al.* [43] observed that 80% of healthy oral epithelial tissues had positive CD44 expression [43]. The lack of significant difference between normal oral mucosa and HCC in terms of CD44 expression does not support the use of CD44 as a single marker in dysplasia and oral cancer.

In our study, when we evaluated the effect of Snail expression on E-cadherin, CD133, and CD44 immunoreactivity by both methods (RT-PCR and immunohistochemistry), no significant difference was observed between Snail/high and Snail/low expression cases. Similarly, Zhu *et al.* [44] found that in Snail-treated oral cancer cells (SCC9), there was no significant difference in terms of CD133 compared to control group cells; however, CD44 expression was positive.

Conclusions

Our study findings suggest that CD133 and E-cadherin, which are involved in EMT-CSC interaction, may be promising diagnostic markers of oral cancer progression via an inflammation pathway. We believe that further studies in this field may lead to a better understanding of the pathobiology of CSCs and the development of anti-tumor drugs and therapies that specifically target these cells. The number of cases was a limitation of our study. We also believe that a larger sample size of a prospective study with extended follow-up would be beneficial.

Disclosures

1. Institutional review board statement: The study was approved by the Ethics Committee of Gazi University, approval number: 142/07102013.
2. Assistance with the article: None.
3. Financial support and sponsorship: This research was funded by the Scientific and Technological Research Council of Türkiye (3001 – AR-GE /TÜBİTAK).
4. Conflicts of interest: None.

References

1. Sung H, Ferlay J, Siegel RL, et al. Global cancer statistics 2020: GLOBOCAN estimates of incidence and mortality worldwide for 36 cancers in 185 countries. *CA Cancer J Clin* 2021; 71: 209-249.
2. Slootweg PJ, Eveson JW. Tumors of the oral cavity and oropharynx: introduction. In: *Pathology and Genetics of Head and Neck Tumours*. Barnes L, Eveson JW, Reichart P, Sidransky D (eds.). Lyon: IARC Press; 2005.
3. Bagan JV, Scully C. Recent advances in oral oncology 2008; squamous cell carcinoma aetiopathogenesis and experimental studies. *Oral Oncol* 2009; 45: e45-e48. DOI: 10.1016/j.oraloncology.2008.12.012.
4. Grizzle WE, Srivastava S, Manne U. The biology of incipient, pre-invasive or intraepithelial neoplasia. *Cancer Biomark* 2010; 9: 21-39.
5. Tsantoulis PK, Kastrinakis NG, Tourvas AD, et al. Advances in the biology of oral cancer. *Oral Oncol* 2007; 43: 523-534.
6. Chang SS, Califano J. Current status of biomarkers in head and neck cancer. *J Surg Oncol* 2008; 97: 640-643.
7. Kobayashi T, Maruyama S, Abe T, et al. Keratin 10-positive orthokeratotic dysplasia: a new leucoplakia-type precancerous entity of the oral mucosa. *Histopathology* 2012; 61: 910-920.
8. Reya T, Morrison SJ, Clarke MF, Weissman IL. Stem cells, cancer, and cancer stem cells. *Nature* 2001; 414: 105-111.
9. Richard V, Pillai MR. The stem cell code in oral epithelial tumorigenesis: 'the cancer stem cell shift hypothesis'. *Biochim Biophys Acta* 2010; 1806: 146-162.
10. Zhang Z, Filho MS, Nor JE. The biology of head and neck cancer stem cells. *Oral Oncol* 2012; 48: 1-9.
11. Bonnet D, Dick JE. Human acute myeloid leukemia is organized as a hierarchy that originates from a primitive hematopoietic cell. *Nat Med* 1997; 3: 730-737.
12. Gonzalez-Moles MA, Scully C, Ruiz-Avila I, Plaza-Campillo JJ. The cancer stem cell hypothesis applied to oral carcinoma. *Oral Oncol* 2013; 49: 738-746.
13. Ishizawa K, Rasheed ZA, Karisch R, et al. Tumor-initiating cells are rare in many human tumors. *Cell Stem Cell* 2010; 7: 279-282.
14. Gale N, Poljak M, Zidar N. Update from the 4th edition of the World Health Organization classification of head and neck tumours: what is new in the 2017 WHO blue book for tumours of the hypopharynx, larynx, trachea and parapharyngeal space. *Head Neck Pathol* 2017; 11: 23-32.
15. Kujan O, Oliver RJ, Khattab A, et al. Evaluation of a new binary system of grading oral epithelial dysplasia for prediction of malignant transformation. *Oral Oncol* 2006; 42: 987-993.
16. Watanabe K, Petro BJ, Shlimon AE, Unterman TG. Effect of periodontitis on insulin resistance and the onset of type 2 diabetes mellitus in Zucker diabetic fatty rats. *J Periodontol* 2008; 79: 1208-1216.
17. Chuhan S, Kitkumthorn N, Satayavivad J. Identification of potential molecular mechanisms and prognostic markers for oral squamous cell carcinoma: a bioinformatics analysis. *J Int Soc Prev Community Dent* 2023; 13: 237-246.
18. Ma J, Wu R, Chen Z, et al. CD44 is a prognostic biomarker correlated with immune infiltrates and metastasis in clear cell renal cell carcinoma. *Anticancer Res* 2023; 43: 3493-3506.
19. Gao J, Li X, Li D, et al. Quantitative immunohistochemistry (IHC) analysis of biomarker combinations for human esophageal squamous cell carcinoma. *Ann Transl Med* 2021; 9: 1086. DOI: 10.21037/atm-21-2950.
20. Barzegar Behrooz A, Syahir A, Ahmad S. CD133: beyond a cancer stem cell biomarker. *J Drug Target* 2019; 27: 257-269.
21. Ong ML, Schofield JB. Assessment of lymph node involvement in colorectal cancer. *World J Gastrointest Surg* 2016; 8: 179-192.
22. Morais EF, Pinheiro JC, Lira JA, et al. Prognostic value of the immunohistochemical detection of epithelial-mesenchymal transition biomarkers in oral epithelial dysplasia: a systematic review. *Med Oral Patol Oral Cir Bucal* 2020; 25: e205-e216. DOI: 10.4317/medoral.23305.
23. Romano M, Francesco FDE, Zarantonello L, et al. From inflammation to cancer in inflammatory bowel disease: molecular perspectives. *Anticancer Res* 2016; 36: 1447-1460.
24. Chen SH, Hsiao SY, Chang KY, Chang JY. New insights into oral squamous cell carcinoma: from clinical aspects to molecular tumorigenesis. *Int J Mol Sci* 2021; 22: 2252. DOI: 10.3390/ijms22052252.
25. Loercher A, Lee TL, Ricker JL, et al. Nuclear factor-kappaB is an important modulator of the altered gene expression profile and malignant phenotype in squamous cell carcinoma. *Cancer Res* 2004; 64: 6511-6523.
26. Wu T, Hong Y, Jia L, et al. Modulation of IL-1beta reprogrammes the tumor microenvironment to interrupt oral carcinogenesis. *Sci Rep* 2016; 6: 20208. DOI: 10.1038/srep20208.
27. Zhang Z, Xu J, Liu B, et al. Ponicidin inhibits pro-inflammatory cytokine TNF-alpha-induced epithelial-mesenchymal transition and metastasis of colorectal cancer cells via suppressing the AKT/GSK-3beta/Snail pathway. *Inflammopharmacology* 2019; 27: 627-638.
28. Glasgow SC, Bleier JIS, Burgart LJ, et al. Meta-analysis of histopathological features of primary colorectal cancers that predict lymph node metastases. *J Gastrointestinal Surg* 2012; 16: 1019-1028.
29. Wang C, Huang H, Huang Z, et al. Tumor budding correlates with poor prognosis and epithelial-mesenchymal transition in tongue squamous cell carcinoma. *J Oral Pathol Med* 2011; 40: 545-551.
30. Takkunen M, Grenman R, Hukkanen M, et al. Snail-dependent and -independent epithelial-mesenchymal transition in oral squamous carcinoma cells. *J Histochem Cytochem* 2006; 54: 1263-1275.

31. Birchmeier W, Behrens J. Cadherin expression in carcinomas: role in the formation of cell junctions and the prevention of invasiveness. *Biochim Biophys Acta* 1994; 1198: 11-26.
32. Nieto MA. The snail superfamily of zinc-finger transcription factors. *Nat Rev Mol Cell Biol* 2002; 3: 155-166.
33. Prall F. Tumour budding in colorectal carcinoma. *Histopathology* 2007; 50: 151-162.
34. Hirohashi S. Inactivation of the E-cadherin-mediated cell adhesion system in human cancers. *Am J Pathol* 1998; 153: 333-339.
35. Rosivatz E, Becker I, Specht K, et al. Differential expression of the epithelial-mesenchymal transition regulators snail, SIP1, and twist in gastric cancer. *Am J Pathol* 2002; 161: 1881-1891.
36. Wicki A, Christofori G. The potential role of podoplanin in tumour invasion. *Br J Cancer* 2007; 96: 1-5.
37. Kumamoto H, Ohki K. Detection of CD133, Bmi-1, and ABCG2 in ameloblastic tumors. *J Oral Pathol Med* 2010; 39: 87-93.
38. Joshua B, Kaplan MJ, Doweck I, et al. Frequency of cells expressing CD44, a head and neck cancer stem cell marker: correlation with tumor aggressiveness. *Head Neck* 2012; 34: 42-49.
39. Ravindran G, Devaraj H. Aberrant expression of CD133 and musashi-1 in preneoplastic and neoplastic human oral squamous epithelium and their correlation with clinicopathological factors. *Head Neck* 2012; 34: 1129-1135.
40. Oliveira LR, Castilho-Fernandes A, Oliveira-Costa JP, et al. CD44+/CD133+ immunophenotype and matrix metalloproteinase-9: influence on prognosis in early-stage oral squamous cell carcinoma. *Head Neck* 2014; 36: 1718-1726.
41. Payne SH. The utility of protein and mRNA correlation. *Trends Biochem Sci* 2015; 40: 1-3.
42. Awasthi S, Ahmad S, Gupta R, et al. Differential expression of cancer stem cell markers and pro-inflammatory cytokine IL-1beta in the oral squamous cell carcinoma and oral submucosal fibrosis. *Int J Health Sci (Qassim)* 2023; 17: 28-38.
43. Margaritescu C, Pirici D, Simionescu C, Stepan A. The utility of CD44, CD117 and CD133 in identification of cancer stem cells (CSC) in oral squamous cell carcinomas (OSCC). *Rom J Morphol Embryol* 2011; 52 (3 Suppl): 985-993.
44. Zhu LF, Hu Y, Yang CC, et al. Snail overexpression induces an epithelial to mesenchymal transition and cancer stem cell-like properties in SCC9 cells. *Lab Invest* 2012; 92: 744-752.

Address for correspondence:

Prof. Sibel E. Gültekin
Department of Oral Pathology
Faculty of Dentistry
Gazi University
Ankara, Turkey
e-mail: sibelg@gazi.edu.tr